European Journal of Medicinal Chemistry 89 (2015) 340–348

Contents lists available at ScienceDirect

European Journal of Medicinal Chemistry

journal homepage: http://www.elsevier.com/locate/ejmech

Original article

Inhibition of pseudolysin and thermolysin by hydroxamate-based MMP inhibitors

Olayiwola A. Adekoya [a, *, 1], Stian Sjøli [b, 1], Yimingjiang Wuxiuer [b], Irina Bilto [a], Sérgio M. Marques [c], M. Amélia Santos [c], Elisa Nuti [d], Giovanni Cercignani [e], Armando Rossello [d], Jan-Olof Winberg [b], Ingebrigt Sylte [b, *]

[a] Department of Pharmacy, Faculty of Health Sciences, UiT – The Arctic University of Norway, NO-9037 Tromsø, Norway
[b] Department of Medical Biology, Faculty of Health Sciences, UiT – The Arctic University of Norway, NO-9037 Tromsø, Norway
[c] Centro de Química Estrutural, Instituto Superior Técnico, Universidade de Lisboa, Av. Rovisco Pais 1, 1049-001 Lisboa, Portugal
[d] Dipartimento di Farmacia, Università di Pisa, Via Bonanno 6, 56126 Pisa, Italy
[e] Dipartimento di Biologia, Unità di Biochimica, Università di Pisa, Via San Zeno 51, 56127 Pisa, Italy

ARTICLE INFO

Article history:
Received 19 December 2013
Received in revised form
30 September 2014
Accepted 4 October 2014
Available online 18 October 2014

Keywords:
Pseudolysin
Thermolysin
Matrix metalloproteinase
Enzyme inhibitors
Docking and scoring

ABSTRACT

In the present study, we have investigated the inhibition of thermolysin and pseudolysin by a series of compounds previously identified as matrix metalloproteinase (MMP) inhibitors using experimental binding studies and theoretical calculations. The experimental studies showed that some of the compounds were able to inhibit thermolysin and pseudolysin in the low μM range. The studies revealed that, in general, the compounds bound in the order MMPs > pseudolysin > thermolysin, and the strongest pseudolysin and thermolysin binders were compounds **8**–**12**. Furthermore, compounds **8** and **9** were unique in that they bound much stronger to the two bacterial enzymes than to the MMPs. The docking calculations suggested that the phenyl group of the strongest binders (compounds **8** and **9**) occupy the S_2'-subpocket, while a second ring system occupy the S_1-subpocket in both thermolysin and pseudolysin. When the compounds possess two ring systems, the largest and most electron rich ring system seems to occupy the S_1-subpocket.

1. Introduction

Thermolysin and pseudolysin belong to the M4 family of metalloproteinases, and are found in bacteria, fungi and archaea. They are both endopeptidases being active at neutral pH (http://merops.sanger.ac.uk) [1]. The prototype enzyme of the family is thermolysin from *Bacillus thermoproteolyticus*, and the family is also termed the thermolysin family. Available three dimensional structures show that they have a catalytic zinc ion at the active site cleft with a tetrahedral coordination formed by the two histidines of a HEXXH motif, and a glutamic acid located 18–72 residues C-terminal of the HEXXH motif. The glutamic acid of the HEXXH motif is catalytically important [2–4]. The fourth zinc coordinating ligand in the free enzymes is a water molecule. Upon inhibitor binding this water molecule is replaced by a metal binding group of the inhibitor [5]. Thermolysin and pseudolysin belong to subclan MA(E) of peptidases, also known as the "Glu-zincins". Matrix metalloproteinases (MMPs) is a family of zinc-containing endoproteinases with broad substrate specificity and extracellular matrix components are among the substrates. MMPs belong to the subclan MA(M), also known as the "Met-zincins" due to the presence of the unique methionine turn close to the ligand binding pocket. In MMPs, the third zinc ligand is a histidine located in the extended motif **H**EXX**H**XXGXX**H**. The presence of the conserved Gly within this motif is necessary for forming the β turn that brings all the three zinc ligating amino acids in close proximity for zinc binding.

Proteinases play important roles in regulating many biological processes including digestion, matrix remodelling and immunity. Proteinase inhibitors are putative drug candidates in several diseases, and are currently under development for treatment of parasitic, bacterial and viral infections, cancer, neurodegenerative

Abbreviations: MMP, Matrix metalloproteinase; MD, Molecular dynamics simulations (Abz: o-aminobenzoyl); AGLA, Abz-Ala-Gly-Leu-Ala-p-nitrobenzylamide; BLS, Bradykinin-like substrate; DMSO, Dimethyl sulfoxide; ICM, The Internal Coordinate Mechanics; PMF, Potential of mean force.

* Corresponding authors.
E-mail addresses: layiadekoya@gmail.com (O.A. Adekoya), Ingebrigt.Sylte@uit.no (I. Sylte).

[1] The two first authors have contributed equally to this work.

http://dx.doi.org/10.1016/j.ejmech.2014.10.009
0223-5234/

diseases, cardiovascular and autoinflammatory diseases [6]. Thermolysin and pseudolysin and other M4 family members are important enzymes for suppressing or avoiding the innate immune response of the infected host during pathogenesis and are putative drug targets in the treatment of bacterial infections [7–13].

Most of the M4 family members are virulence factors secreted from Gram-positive or Gram-negative bacteria that degrade extracellular proteins and peptides used for bacterial nutrition prior to sporulation. The family includes enzymes from pathogens such as *Legionella*, *Listeria*, *Clostridium*, *Staphylococcus*, *Pseudomonas* and *Vibrio* [4,14], and family members have been implicated as key factors in various disease conditions [14,15]. The contribution to disease may be directly by tissue destruction and damage of the cell function, or indirectly by interfering with the host-defence mechanism by impairing normal function of host proteinases. The thermolysin like proteinases from *Helicobacter pylori* and *Vibrio cholerae* are involved in the bacterial pathogenesis and contribute to the development of gastritis, peptic ulcer, gastric carcinoma [16] and cholera [17]. The thermolysin like proteinase from *Legionella* is suggested to be involved in Legionaire's disease and pneumonia [18]. Pseudolysin has muscle damaging effects and severe hemorrhagic activity [19], and is involved in the development of lung infections [20–23]. Several studies indicate that pseudolysin is involved in the development of chronic ulcers by degradation of proteins and peptides in human wound fluids and skin [24]. Pseudolysin is also implicated in corneal infections, causing sight threatening corneal liquefaction [25]. Therapeutic inhibition of enzymes of the M4 family is therefore believed to be a novel strategy in the development of second-generation antibiotics. However, the inhibitors should not interfere with human proteinases like the matrix metalloproteinases (MMPs). The catalytic Zn^{2+} of both the MMPs and the M4 enzymes is surrounded by subsite pockets with large structural similarities. Designing inhibitors of therapeutic value that can distinguish between M4 enzymes and MMPs is challenging. It is therefore important to identify structural determinants for high affinity binding to the bacterial M4 enzymes and to the different endogenous zinc proteinases such as the MMPs.

We have previously studied the inhibition of M4 family enzymes using theoretical calculations and experimental binding studies [26–29]. In the present work we studied a series of compounds (Fig. 1.) previously found to inhibit one or more MMPs [30–33] as putative inhibitors of thermolysin and pseudolysin using experimental binding studies and molecular modelling studies. The inhibitors were docked into the active site of pseudolysin, thermolysin, MMP-1, MMP-2, MMP-9 and MMP-14. There are several thermolysin-inhibitor complexes in the PDB database, and the docking indicated that the tested compounds bound thermolysin quite similar to known thermolysin inhibitors. Few complexes of pseudolysin with an inhibitor that could be used to evaluate the docking poses were found in the PDB database. The stability of the pseudolysin docking poses was therefore tested by 24 ns of molecular dynamics (MD) simulations. For the MMPs, several inhibitor complexes were found in the PDB database that could be used to evaluate the docking poses.

2. Results and discussion

2.1. Biological activity of isolated enzymes

The structures of the tested compounds are shown in Fig. 1. The IC_{50} values determined from the enzyme inhibition studies indicated that the tested compounds bind, in general, slightly stronger to pseudolysin than to thermolysin (Table 1). The experimental results revealed that the best pseudolysin binders were compounds **1** and **8**–**12** with the IC_{50} values ranging from 0.4 (±0.3) to 31 (±13) μM when using the AGLA substrate (Table 1). Two substrates were used for the studies because of solubility issues.

Compounds **1**, **8** and **9** are weak MMP inhibitors with IC_{50} values larger than 100 μM. Compounds **8** and **9** bind significantly stronger to the M4 enzymes than to the MMPs (Table 1). The rank order of binding of compound **1** was pseudolysin > MMPs > thermolysin. In general, the other tested compounds bound stronger to the MMPs than to the M4 enzymes. However, compounds **2**, **3** and **7** were quite weak MMP-binders (Table 1). Of the best pseudolysin binders compounds, **8**, **10** and **12** were also tested for using the BLS substrate. The main difference was that compound **12** bound weaker when using the BLS substrate (IC_{50} 16 ± 2 μM vs. 276 ± 18 μM). This may reflect differences in the experimental conditions or in the protein binding modes between the BLS and AGLA substrates. There were also differences in IC_{50} for other inhibitors when using the AGLA and BLS substrates (Table 1). Brij-35 was used in the binding studies with BLS for both thermolysin and pseudolysin, but not with AGLA for pseudolysin. Previous studies have shown that Brij-35 may affect catalytic activity and inhibition of proteinases [34].

The structural similarities in the catalytic region of the different zinc metalloproteinases are large and specificity is therefore a problem in the development of drugs targeting these enzymes. In spite of that, the zinc metalloproteinases are able to discriminate between many possible substrates and to cleave at specific sites. Thermolysin and pseudolysin preferentially cleave at the N-terminal side of hydrophobic amino acids occupying the S_1' binding pocket [4,5]. The substrate specificity is mostly determined by subsites that are important for recognition and correct orientation of the given substrate at the binding site. In order for an inhibitor to discriminate between proteinases, it is reasonable to believe that the subsite occupation is important. The binding studies for

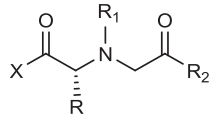

SPE = -CH_2CH_2-(C$_6$H$_4$)-SO_2NH_2

PIP = piperazine

	X	R	R_1	R_2
1	NHOH	H	-CH_2PhNO_2	OH
2	NHOH	H	-CH_2PhPh	OH
3	NHOH	H	-CH_2PhOPh	OH
4	NHOH	H	-SO_2PhOCH_3	OH
5	NHOH	H	-SO_2PhPh	OH
6	NHOH	H	-SO_2PhOPh	OH
7	NHOH	H	-$NH(CH_2)_3PipPh$	OH
8	NHOH	H	-CH_2Ph	-$NH(CH_2)_3PipPh$
9	NHOH	H	-CH_2Ph	-NHSPE
10	NHOH	H	-SO_2PhOCH_3	-NHSPE
11	NHOH	H	-SO_2PhPh	-NHSPE
12	NHOH	H	-SO_2PhOPh	-NHSPE
13	NHOH	*i*-Pr	-SO_2PhOPh	OH
14	OH	H	-SO_2PhOCH_3	-NHSPE

Fig. 1. The 2D structures of the tested compounds.

Table 1
The obtained IC_{50} values for thermolysin and pseudolysin and previously published IC_{50} values of the compounds for MMP-1, MMP-2, MMP-9 and MMP-14. The IC_{50} values for pseudolysin were measured with two different substrates. AGLA: the substrate Abz-Ala-Gly-Leu-Ala-p-nitrobenzylamide. BLS: the bradykinin like substrate. ND: not determined. All IC_{50} values are given in μM.

Compound	Thermolysin	Pseudolysin		MMP-1	MMP-2	MMP-9	MMP-14
	BLS	BLS	AGLA				
1	755 ± 17	ND	20 ± 2	ND	178±6[a]	>300[a]	313 ± 25[a]
2	>1000	ND	>121	ND	79±7[a]	70.8 ± 0.9[a]	116±5[a]
3	524 ± 64	430 ± 123	>200	ND	238 ± 18[a]	74.6 ± 0.93[a]	138 ± 3.5[a]
4	270 ± 40	153 ± 5	169 ± 8	6.8 ± 0.6[a]	0.19 ± 0.02[a]	0.32 ± 0.03[a]	1.7 ± 0.2[a]
5	440 ± 46	241 ± 14	>150	2.6 ± 0.3[a]	0.046 ± 0.002[a]	0.155 ± 0.005[a]	1.42 ± 0.08[a]
6	114 ± 10	46 ± 4	>186	1.53 ± 0.06[a]	0.0012 ± 0.0001[a]	0.0032 ± 0.0002[a]	0.030 ± 0.002[a]
7	>1000	ND	>330	ND	234±5[a]	>300[a]	172±7[a]
8	8 ± 1	2.8 ± 0.2	6.7 ± 0.5	ND	>300[a]	>300[a]	>300[a]
9	12 ± 1	ND	0.4 ± 0.3	ND	>100[b]	>300[b]	>100[b]
10	164 ± 22	33 ± 2	15 ± 2	0.53 ± 0.02[b]	0.025 ± 0.002[b]	0.054 ± 0.003[b]	0.090 ± 0.004[b]
11	67 ± 4	ND	31 ± 13	0.54 ± 0.02[b]	0.016 ± 0.001[b]	0.066 ± 0.006[b]	0.26 ± 0.02[b]
12	160 ± 31	276 ± 18	16 ± 2	0.14 ± 0.01[b]	0.0016 ± 0.0003[b]	0.00051 ± 0.00004[b]	0.0021 ± 0.0002[b]
13	>1000	336 ± 34	82 ± 12	0.059 ± 0.004[b]	0.0005 ± 0.0002[b]	0.00077 ± 0.00005[b]	0.0039 ± 0.0003[b]
14	637 ± 39	ND	>282				

[a] From Ref. [33].
[b] From Ref. [31].

pseudolysin were performed with two different substrates (AGLA and BLS). Table 1 shows that the IC_{50} values of the compounds varied slightly with the substrates used.

2.2. Theoretical predictions of enzyme–ligand interactions

The ICM docking indicated the compounds have quite similar binding modes in pseudolysin and thermolysin. However, for the weaker thermolysin inhibitors with a carboxyl group (OH in R_2) (Fig. 1) clear trends in docking poses were not seen. The docking showed that the compounds had orientations quite similar to each other in thermolysin and pseudolysin and that their binding poses also were quite similar to inhibitors in known X-ray structure complexes of thermolysin and pseudolysin. This is illustrated in Fig. 2 where the docking modes of compounds **8** and **9** are compared with the binding pose of the carboxylate inhibitor of the 1u4g complex of pseudolysin from the PDB-database (Fig. 2A). However, compounds **8** and **9** could penetrate deeper into S_1 − subpocket than the inhibitor of the 1u4g complex. However, quite few complexes of pseudolysin with inhibitors are present in the PDB-database, and the structural stability of the docked complexes was therefore tested by MD-simulations. The MD simulations showed that the complexes were robust, and that the inhibitor docking poses remained stable during the MDs. Amino acids within 4 Å of the inhibitors in the average complexes between 20 and 24 ns of MD are shown in Table 2. This table indicates that all the inhibitors occupy the same regions in pseudolysin.

2.2.1. Binding of the inhibitors to pseudolysin and thermolysin

The X-ray crystal structure complexes of thermolysin and pseudolysin show that the overall geometry of the binding pocket for small molecules can be divided into three subpockets:

- The S_1'-subpocket, the main subpocket for substrate recognition which accommodates quite selectively hydrophobic amino acids both in thermolysin and pseudolysin.
- The S_2'-subpocket, also quite hydrophobic.
- The S_1-subpocket, larger and more hydrophilic than the other subpockets.

Except for compound **1**, the hydroxamate derivatives containing a carboxylic group (compounds **2**–**7** and **13**) revealed to be quite weak pseudolysin binders. The theoretical studies showed that

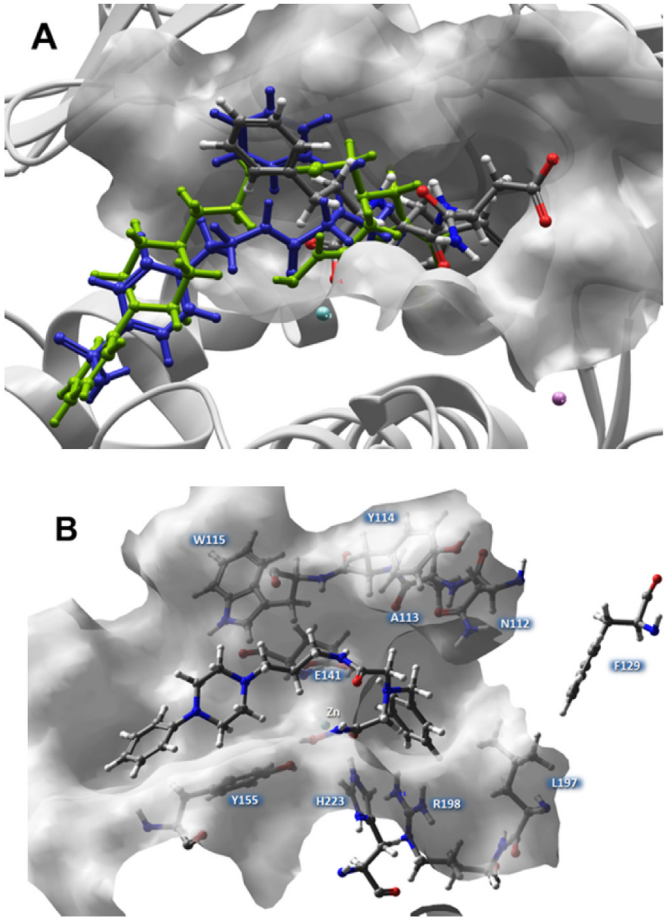

Fig. 2. A: Compound **8** and **9** superimposed onto the inhibitor of the pseudolysin-inhibitor complex 1u4g in the PDB database. Semi-transparent solid skin surface representation has been used to illustrate the ligand binding pocket. Colour coding: Compound 8; green, compound 9; blue; the inhibitor of the 1u4g complex; grey, zinc ion; light blue, one calcium ion; pink. B: A close up of compound **8** in the binding site of pseudolysin. The most important amino acids for binding the compounds are shown in the figure. The S_1-subpocket is in the region of W115/Y155, while the S_2'-subpocket is in the region of N112/R198. Colour coding of atoms: red; oxygen, blue; nitrogen, grey; carbon, white; hydrogen, light blue; zinc ion.

Table 2
Amino acids within 4 Å from the ligand in the average inhibitor-pseudolysin complexes calculated between 20 and 24 ns of MD.

Compound	Amino acids within 4 Å of the ligand
1	A113, Y114, H140, E141, H144, Y155, E164, L197, R198, R208, H223, Zn
2	Y114, H140, E141, H144, L153, Y155, G160, N163, E164, V222, H223
3	H140,E141, H144, G145, E148, Y155, E164, V222, Zn
4	Y114, W115, D116, G117, H140, E141, H144, Y155, E164, Zn
5	Y114, W115, H140, E141, H144, Y155, E164, V222, H223, Zn
6	Y114, H140, E141, H144, Y155, E164, V222, Zn
7	H140, E141, H144, Y155, R156, E164, V222, H223, Zn
8	N112, A113, Y114, W115, H140, E141, H144, T147, E148, Y155, G160, N163, E164, L197, R198, V222, H223, Zn
9	N112, A113, Y114, W115, D116, G117, H140, E141, H144, G145, E148, Y155, N163, E164, L197, R198, V222, H223, Zn
10	A113, Y114, W115, D116, G117, M120, V137, H140, E141, H144, Y155, E164, I186, L197, R198, V222, H223
11	N112, A113, M120, D136, V137, A138, H140, E141, H144, E164, D168, I186, L197, R198, H223, Zn
12	Y114, W115, H140, E141, H144, T147, E148, Y155, E164, V222, H223
13	W115, H140, E141, H144, E148, G152, L153, I154, Y155, N163, E164, V222, Zn
14	A113, Y114, W115, H140, E141, H144, E148, Y155, E164, V222, H223, Zn

these compounds occupied the S_1-and S_1'-subpockets of pseudolysin with the aromatic ring systems in between the side chains of Trp115 and Tyr155 in the S_1-pocket. Compound **1**, the strongest binder among the compounds with a carboxylic group, occupied the S_1'- and S_2'-subpockets with the aromatic ring system in the S_2'-subpocket having strong interactions with Asn112 and Arg198. The compound also interacted strongly with His140. That mode of binding gave favourable interactions with the zinc ion, and strong electrostatic interactions with the enzyme. The docking indicated that the aromatic group of the compounds with a carboxylic group enters the S_2'-subpocket when the group is small enough. When the group is larger and/or more electron rich (as in compounds **2**–**7** and **13**), the group enters the S_1-subpocket which is wider and more hydrophilic. In thermolysin the compounds with a carboxylic group were quite weak binders and not easy to dock in proper poses, and clear trends were not seen. For the compounds with a carboxyl group, poses both with the ring system in the S_1- and in S_2'-subpocket were observed.

The best pseudolysin binders were compounds **1**, **8**–**12** (Table 1). In compounds **8**–**12**, the carboxylic group that is present in compound **1** has been replaced by a moiety containing an aromatic ring system (Fig. 1). For the strongest binders (compounds **8** and **9**), the predictions indicated that this ring system occupies the S_1-subpocket, giving interactions with Trp115 and Tyr155, the phenyl ring interacts in the S_2'-subpocket obtaining interactions with Asn112 and Arg198, while the hydroxamate group has very favourable interactions with the zinc ion (Fig. 2B). However, when the ring system corresponding to the phenyl group in compounds **8** and **9** is larger (as for compounds **10**–**12** and **14**) the pocket becomes too narrow for a proper accommodation of the ring system, and it occupies the S_1-subpocket, which is larger and more hydrophilic. These results indicate that when the compound has more than one ring system, the biggest and most electron rich ring system occupies the S_1-subpocket of pseudolysin. Compounds **8** and **9** are also the best thermolysin binders among these compounds, and docking indicated that their binding pose in thermolysin is quite similar to that in pseudolysin. The docking studies of the compounds into thermolysin show that both compounds **8** and **9** had hydrophobic contacts with amino acids Phe130 (Phe129 in pseudolysin), Leu202 (Leu197 in pseudolysin), Val192 (Ile190 in pseudolysin), and Leu133 (Leu132 in pseudolysin). Such interactions are also observed in the X-ray crystal structures complexes of thermolysin with inhibitors. Furthermore, compounds **8** and **9** had hydrogen bond interactions with Arg203 (Arg198 in pseudolysin), Glu143 (Glu141in pseudolysin) and Asn112 (Asn112 in pseudolysin) (Table 2). Both compounds **8** and **9** also had π−cation interactions with Arg203 in thermolysin. In order to test the importance of the hydroxamate group for zinc coordination and ligand binding, we also tested compound **14**. Compounds **14** and **10** are similar except for that the hydroxamate group is replaced with a carboxylic acid in compound **14**. The latter compound had very low affinity for both thermolysin and pseudolysin compared with compound **10**, which show that the hydroxamate is very important for zinc coordination and binding, as previously suggested.

2.2.2. Difference in binding between the M4 enzymes and the MMPs

From our point of view compounds **8** and **9** are very interesting since they bind stronger to the bacterial enzymes than to the MMPs. As previously explained, the interactions with amino acids within the subpockets S_1 and S_2' were the main contribution to their quite strong binding to thermolysin and pseudolysin (Table 1). The calculations also indicated that compounds **8** and **9** (Fig. 2B) formed aromatic interactions with (pseudolysin numbering): Tyr114 (Phe in thermolysin), Trp115, Phe129, Tyr155 (Table 2). This region contains amino acids both within the S_1- and S_2'-subpocket of the bacterial enzymes. However, in this region there are important structural differences between the bacterial enzymes and the MMPs. Tyr/Phe114 and Trp115 (pseudolysin numbering) is in a β-sheet structure. In the MMPs this region has not a clear secondary structure and the MMPs have a leucine in this region that is lacking in the bacterial enzymes (highlighted in Fig. 3). In the MMPs, this leucine (L188) is protruding into the binding pocket (Fig. 4). The tyrosine (Y423) corresponding to Tyr177 in pseudolysin is also highlighted in Fig. 3. This tyrosine is conserved between the MMPs and thermolysin/pseudolysin. However, the structural alignment of the enzymes indicated that the three dimensional structures are different in this region. In the bacterial enzymes the tyrosine is located in an α-helix, while it is located in a loop in the MMPs. This loop is closer to the active site than the corresponding α-helix in the bacterial enzymes. As the leucine side chain, the tyrosine side chain is also protruding into the binding pocket. The structural differences in the region corresponding to Tyr114/Trp115 and Tyr177 (Fig. 3) contribute to structural differences both in the S_1- and S_2'-subpockets between pseudolysin/thermolysin on one side and MMP-1, -2, -9 and 14 on the other side.

In addition, the leucine that is not present in the bacterial enzymes and the tyrosine corresponding to Tyr177 of pseudolysin are protruding into the binding pocket of the MMPs and contribute to a very narrow access to the subpocket S_1' in the MMPs compared to thermolysin and pseudolysin (Fig. 4). The observed structural differences seem to affect the interactions of compound **8** and **9** with amino acids within subpockets S_1 and S_2' and contribute to the low affinity of compounds **8** and **9** for these MMPs. Binding poses similar to those in thermolysin and pseudolysin were not obtained when docking compounds **8** and **9** into MMP-1, -2, -9 and -14.

Docking of the compounds into the MMPs showed that the high affinity binders, like compound **12** and **13**, interact with the MMPs at the top of subpocket S_1' but did not enter into the S_1'-subpocket due to the hindrance caused by the leucine and the tyrosine (Leu188 and Tyr423 in MMP-9). In MMP-9, the S_1'-subpocket consists of the region Leu418, Tyr423, Arg424 and Phe425. A similar

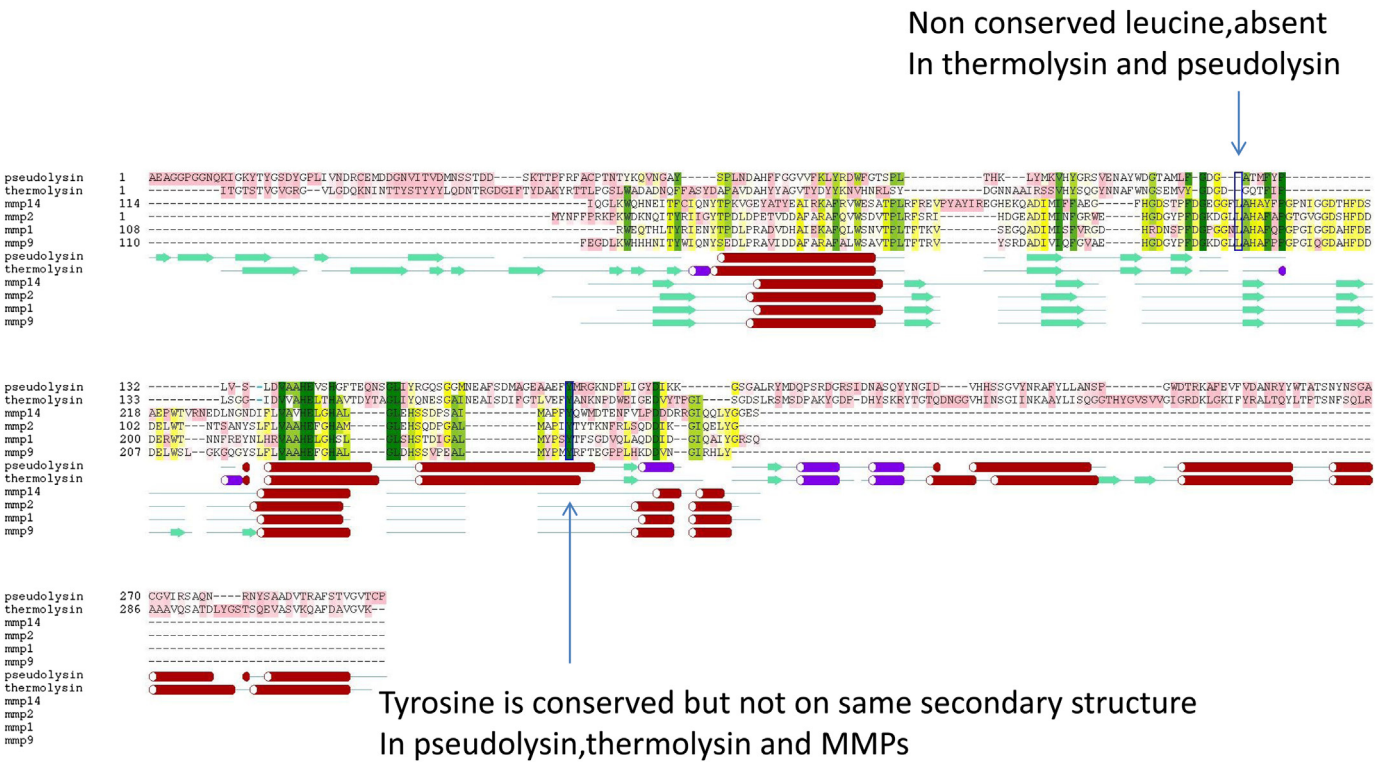

Fig. 3. Multiple sequence and structure alignment of pseudolysin, thermolysin, MMP-1 (PDB-code: 966c), MMP-2 (PDB-code: 1hov), MMP-9 (PDB-code: 1gkc) and MMP-14 (PDB-code: 1bqq), pseudolysin (PDB-code: 1u4g) and thermolysin (PDB-code: 1pe5). The boxed sequences show the region of the sequentially conserved tyrosine and the region of the leucine residue that is conserved in MMPs but not in pseudolysin and thermolysin. The tyrosine is situated on a helix in thermolysin and pseudolysin but on a loop in the MMPs.

mode of binding is also seen in most of the X-ray crystal structures of MMP-1, -2, and -9 with an inhibitor. However, there are some inhibitors that can enter the narrow S_1'-subpocket, and give strong interactions with the enzymes. This is seen for X-ray complexes of MMP-1 (PDB-code: 966c), MMP-2 (PDB code: 3ayk and 4ayk) and MMP-9 (PDB code: 2owl, active site mutant). Compounds **12** and **13** are very strong inhibitors of MMP-9, and their docking poses are shown in Fig. 4. Compound **13** interacted with MMP-9 by forming hydrogen bonds with main chain amide moieties of Ala189 and Leu188. Compound **13** also had hydrophobic–aromatic interaction with Leu188, Leu397, Leu398, His401 and Leu418. Furthermore, aromatic–aromatic interaction was observed with Tyr420 and Tyr423. Similar interactions were not observed with compounds **8** and **9** that both are weak MMP binders.

The induced fit docking was scored by calculating the potential of mean force (pmf). Pmf calculations provide an independent score of the strength of ligand–receptor interaction. The pmf binding scores for compound **8** were: Pseudolysin, −1079.0; thermolysin, −1063.0; MMP-1, −719.2; MMP-2, −831.3; MMP-9, −721.2; and MMP-14, −640.1. The scores with compound **9** were: Pseudolysin, −1091.0; thermolysin, −1041.6; MMP-1, −764.8; MMP-2, −823; MMP-9, −721.5; and MMP-14, −695.3. These values suggest that the pmf score for compounds **8** and **9** reflected the obtained experimental binding strengths (Table 1). The hydrogen

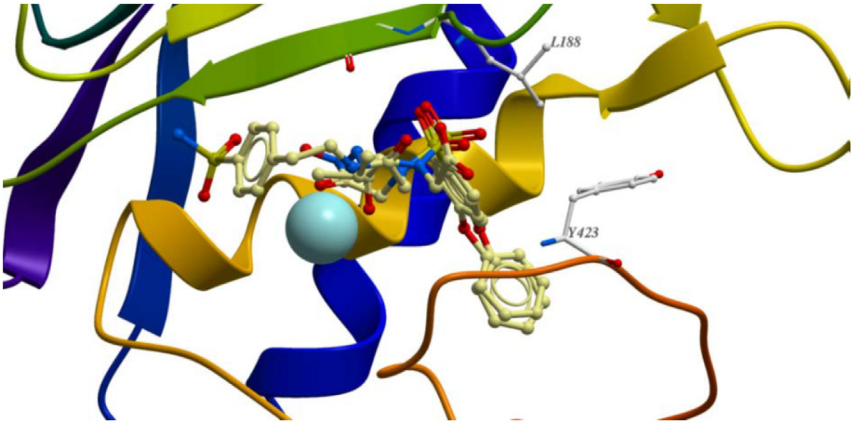

Fig. 4. Superimposed docking complexes of compounds **12** and **13** with MMP-9. The side chains of Leu188 and Tyr423 have been displayed. These amino acids are blocking the entrance of the compounds deeper into subpocket S_1'. Colour coding of ligand atoms: red; oxygen, blue; nitrogen, yellow; carbon, green; sulphur, light blue; zinc ion.

bonding network after induced fit docking showed that both compounds **8** and **9** formed 7 hydrogen bonds with pseudolysin, while the corresponding numbers for thermolysin were 7 and 5, respectively (Table 3). The corresponding numbers for compound **8** with the MMPs were: MMP-1; 4, MMP-2; 1, MMP-9; 3, MMP-14; 3, and for compound **9**: MMP-1; 4, MMP-2; 6, MMP-9; 5, MMP-14; 6. The side chain or the main chain peptide bond of the following amino acids were involved in hydrogen bonding in pseudolysin and thermolysin were (pseudolysin numbering): Ala113, Asn114, Glu141, Arg198, Tyr155 and His223, while in the MMPs the main contribution to hydrogen bonding were from hydrophobic amino acids (Ala, Leu, Phe and Pro) and a few polar and charged amino acids (Glu, Gln and Tyr). The induced fit docking suggested that compounds **8** and **9** formed hydrogen bonds with several side chains of polar and charged amino acids in the bacterial enzymes, while the main contribution to the interactions in the MMPs were with the main chain or side chain of peptide bond of hydrophobic amino acids.

3. Conclusion

In the present work enzyme inhibition studies were used to determine the IC_{50} values of a series of 14 compounds for thermolysin and pseudolysin. These compounds have previously been investigated for their ability to inhibit different MMPs. The molecular interactions of the compounds with MMP-1, MMP-2, MMP-9, MMP-14, thermolysin and pseudolysin were also studied by molecular docking and scoring in order to reveal molecular explanations for their affinity differences. A very promising observation in the present study was that the two compounds **8** and **9** bound much stronger to pseudolysin and thermolysin than to the MMPs. This could be explained by structural differences between the bacterial enzymes and the MMPs in S_1-, S_1'- and S_2'-subpockets and the hydrogen bonding network formed with amino acids at the active site, suggesting that the structures of these compounds are important for further design of new thermolysin and pseudolysin inhibitors with low MMP binding affinity.

In general the compounds bound stronger to pseudolysin than to thermolysin. The strongest pseudolysin binders were those in which the carboxylic group was replaced by a moiety bearing an aromatic ring system (compounds **8**–**10** and **12**). The strongest binders for both thermolysin and pseudolysin were compounds **8** and **9** (IC_{50} values in the low μM to nM range). The docking studies suggested that their phenyl group occupies the S_2'-subpocket, while the other ring system occupies the S_1-subpocket in both thermolysin and pseudolysin. When the compound possesses two ring systems, the largest and most electron rich ring system seems to occupy the S_1-subpocket. The S_1-subpocket is larger and more hydrophilic than the S_2'-subpocket.

Table 3
Amino acids involved in hydrogen bonding with compounds **8** and **9**. The number of hydrogen bonds formed between the amino acid and the compound is given in brackets.

Enzyme	Compound **8**	Compound **9**
Thermolysin	A113(1), N112(2), E143(1), Y157(1), R203(2)	E143(3), Y157(2))
Pseudolysin	A113(1), E141(4), R198(1), H223(1)	E141(5), R198(1), H223(1)
MMP-1	N180(1), L181(1), A182(2)	A181(1), E219(2), T241(1)
MMP-2	E121(1)	L83(1), A84(1), E121(2), A139(1), R149(1)
MMP-9	F101(1), A189(1), A191(1)	E402(3), P430 (1), Y423(1)
MMP-14	E240(2), A203(1)	A200(1), A202(2), A258(1), F260(1), Q262(1)

4. Materials and methods

4.1. Experimental binding studies

The inhibitory activity (in terms of IC_{50} value) for pseudolysin and thermolysin were measured using two different fluorogenic substrates: 1. Abz-Ala-Gly-Leu-Ala-p-nitrobenzylamide (AGLA), (Abz: o-aminobenzoyl). 2. Mca-Arg-Pro-Pro-Gly-Phe-Ser-Ala-Phe-Lys-(Dnp)-OH (Bradykinin-like substrate – BLS), (Mca = (7-methoxycoumarin-4-yl) acetyl; Dnp = 2,4-dinitrophenyl).

4.1.1. Materials

Three times crystallized thermolysin (activity ≥ 7000 units/mg) was from CalBioChem. Pseudolysin was obtained as a gift from Prof. Efrat Kessler, Tel Aviv University Sackler, Israel, and also purchased from CalcBioChem. DMSO was from Merck. AGLA was obtained from Bachem, while the BLS substrate was from AnaSpec (ID: 929-ZN-10). Synthesis of the compounds has been described previously [30–33].

4.1.2. Instrument and instrument settings

To determine the IC_{50} value of the compounds for pseudolysin and thermolysin, initial rate measurements were performed at 37 °C with different instruments and substrates. The instruments and instrument settings were as follows:

4.1.2.1. AGLA. These experiments were performed on either a Perkin Elmer LS 50 Luminescence spectrometer controlled by the FL WinLab Software Package (Perkin Elmer) or a Spectra Max Gemini EM Plate Reader controlled by the computer program Soft Max Pro version 4.3 (Molecular Devices). All assays were performed with an excitation wavelength of 330 nm and an emission wavelength of 460 nm, using slit widths of 10 nm.

4.1.2.2. BLS. Spectra Max Gemini EM Plate Reader controlled by the computer program Soft Max Pro version 4.3 (Molecular Devices) or a Spectra Max Gemini XS (03148, Molecular Devices). All assays were performed with an excitation wavelength of 328 nm and an emission wavelength of 393 nm.

4.1.3. Determination of IC_{50} values using the AGLA substrate

The compounds were dissolved in 100% DMSO and were further diluted with water to give a concentration of 100 μM. The enzyme inhibition studies were performed under a set of different conditions which varied with substrate and enzyme used, as described below.

4.1.3.1. Pseudolysin. The AGLA substrate was dissolved in 50% acetic acid, giving a concentration of 500 μM. 4 μL of 1.0 μM enzyme was preincubated for 15 min at 37 °C with 4 μL of inhibitors (appropriate concentrations) and 100 μL of 0.1 M Tris–HCl, 5 mM $CaCl_2$, pH 8.25 and 88 μL water (Milli-Q). In the controls, the inhibitor solution was substituted with buffer and in the inhibitor and control experiments the final DMSO concentration was less than 5%. The enzyme reaction was started by adding 4 μL of AGLA to the enzyme-inhibition mixture which resulted in a total reaction volume of 200 μL, with final substrate and enzyme concentrations of 10 μM and 20 nM, respectively, and a pH of 7.8. The initial reaction rate was monitored for 1 min. Plots of v_i/v_0 against [I] were used to determine the IC_{50} value where v_i and v_0 represents the initial rate of substrate cleavage in the presence and absence of inhibitor, respectively. Graph Pad Prism 5 was used to determine the IC_{50} value, using equation (1):

$$v_i/v_0 = 1/(1 + [I]/IC_{50}) \quad (1)$$

All experiments were performed in duplicate [35].

4.1.3.2. Thermolysin. A stock solution of 2.0 mM AGLA in 100% DMSO was further diluted to 75 μM in 0.1 M Hepes, pH 7.3, containing 10 mM $CaCl_2$ and 0.005% Brij-35 ($C_{12}H_{25}O(CH_2CH_2O)_{23}H$). Five μL of enzyme solution (4.4 nM) was pre-incubated for 15 min at 37 °C with 10 μL of inhibitors (appropriate concentrations) and 65 μL of 0.1 M Hepes, 10 mM $CaCl_2$, 0.005% Brij-35, pH 7.3. In the controls, the inhibitor was exchanged with buffer. In the inhibitor and control experiments the final DMSO concentration was 5%. The enzyme reaction was started by adding 20 μL of AGLA (75 μM) to the enzyme-inhibition mixture which resulted in a total reaction volume of 100 μL with final substrate and enzyme concentrations of 15 μM and 0.21 nM respectively, and a pH of 7.3. The final inhibitor concentrations in the assays varied from 10^{-3} to 10^{-10} M. The initial rate of the reaction was followed for 30 min at 37 °C. The enzyme kinetic program in Sigma-Plot was used to determine the IC_{50} value and due to the large range of inhibitor concentration, the logarithm of [I] and IC_{50} was used in equation (1) which then results in equation (2):

$$\frac{v_i}{v_0} = \frac{1}{\left(1 + 10^{(pIC_{50} - pI)}\right)} \quad (2)$$

where pI = −log [Inhibitor] in M, pIC_{50} = −log IC_{50} in M. All experiments were performed at least in triplicate.

4.1.4. Determination of IC_{50} values using the BLS substrate

The IC_{50} values were measured both for thermolysin and pseudolysin using BLS as substrate. Thermolysin assay: Hepes buffer (0.1 M, pH 7.5) $CaCl_2$ (10 mM) and Brij-35 (0.005%), substrate (3.33 μM), Thermolysin (5 nM). Pseudolysin assay: Hepes buffer (0.1 M, pH 7.5), $CaCl_2$ (10 mM), NaCl (150 mM) and Brij-35 (0.005%), substrate (1.73 μM), Pseudolysin (5 nM). The substrate-powder was dissolved in DMSO, and diluted two sequential times in assay buffer, so the fixed DMSO contribution with substrate in the assay was 1% in the thermolysin assay and approximately 0.5% in the Pseudolysin assay. The inhibitors were dissolved in DMSO to a stock concentration of 10 mM, and seven inhibitor concentrations were used for each inhibitor ranging from low (typical 0.1–1) to high (500) μM concentration. The DMSO contribution was at most 5%, but was often kept below 1%. Thermolysin remained unaffected by 6% DMSO in our experiments, and therefore the varied DMSO amounts should not affect the outcome. The inhibitors were pre-incubated with free enzyme for 1 h in plate wells at room temperature. Substrate was added before the changes in fluorescence were measured over a period of 15 min. Three parallels were performed for control, where the inhibitor was replaced with buffer. The decrease in rate, due to added inhibitor, was calculated as percentage (%) relative to the controls (Softmax Pro 4.7.1), and analysed with a non-linear curve fitting (Origin 6.0) using equation (1).

4.1.5. Kinetic parameters

Prior to determination of the IC_{50} values of the various inhibitors, it was necessary to determine the K_m values for the two enzymes with AGLA and BLS. Each K_m determination was performed on the Perkin Elmer LS 50 Luminescence spectrometer at 25 °C with AGLA and 37 °C with BLS, using the instrument settings described above for respective substrate. Initial rates were determined with AGLA concentrations ranging from 30 to 400 μM. All assays were performed in Hepes (0.1 M), $CaCl_2$ (10 mM), Brij-35 (0.005%), pH 7.3 with AGLA and pH 7.5 with BLS, using a final concentration of 2.2 nM thermolysin and 5.0 nM pseudolysin. Initial rates of BLS were determined with substrate concentrations ranging from 1.3 to 10.0 μM, while higher substrate concentrations resulted in quenching. At least two independent experiments were performed to obtain reliable K_m values. The K_m values were calculated from non-linear regression of the Michaelis–Menten equation using the Enzyme kinetic module in Sigma Plot.

K_m values of 68 ± 10 and 128 ± 23 μM were obtained for AGLA with Thermolysin and Pseudolysin respectively, while the corresponding values for BLS were 15 ± 3 and 10 ± 3 μM. This resulted in $[S]/K_m$ values of 0.22 and 0.08 for AGLA with Thermolysin and Pseudolysin respectively, while the corresponding values for BLS were 0.11 and 0.17. The relation between K_i and IC_{50} for a substrate competitive inhibitor is $K_i = IC_{50}/(1+[S]/K_m)$. Thus the obtained IC_{50} values for the two enzymes with the two different substrates will reflect the dissociation constant K_i.

4.2. Molecular modelling

4.2.1. Docking

The Internal Coordinate Mechanics (ICM) program [36] was used for docking the inhibitors into the target proteinases. The X-ray crystal structures of a pseudolysin (PDB-code: 1u4g), thermolysin (PDB-code: 1pe5). MMP-1 (PDB-code: 966c), MMP-2 (PDB-code: 1how), MMP-9 (PDB-code: 1gkc) and MMP-14 (PDB-code: 1bqq) were collected from the PDB database. Crystallographic waters were removed along with the co-crystallized small molecule inhibitors and hydrogen atoms were added and optimized using the ECEPP/3 force field of ICM. The various inhibitors were built using ICM and minimized before docking. A grid map that included the active site amino acids was calculated for the enzymes, and semi-flexible docking with flexible ligands were performed.

The binding studies suggested that compound **8** and **9** bound much stronger to pseudolysin and thermolysin than to the MMPs. In order to look for a molecular explanation, these compounds were also studied by induced fit docking into the bacterial enzymes and the MMPs using the ICM software. Induced fit docking is an extension of the traditional flexible ligand–rigid target docking approach. In induced fit docking an initial regular flexible ligand/–rigid protein docking is performed to generate an ensemble of ligand poses, followed by MD force-field based sampling of the structure of the amino acids at the binding site. During this sampling, both the backbone and side chains are free to move. The ligand is then re-docked and scored. The induced fit docking was scored by calculating the pmf.

4.2.2. Molecular dynamics simulation of pseudolysin-ligand interactions

Amber 9.0 was used for molecular dynamics simulations of pseudolysin–ligand interactions [37]. MD simulations of the pseudolysin-inhibitor interactions were performed as a test of the robustness and stability of the inhibitor binding poses obtain by docking into pseudolysin. The complexes after docking were used as starting structures for 24 ns simulations. Before simulations, the electrostatic potentials of each inhibitor were calculated using the antechamber program of the Amber suit of programs and the inbuilt AMI-BCC charges [38,39]. The electrostatic potentials were used to derive atomic restrained electrostatic point (RESP) charges of the inhibitors [40,41]. A non-bonded approach was used for the metal ions [42–45]. Zinc was assigned a formal charge of +2.0, van der Waals' radius 0.69 Å and well depth $\varepsilon = 0.014$ kcal/mol. Calcium was assigned a formal charge of +2.0, van der Waals' radius 1.6 Å and well depth $\varepsilon = 0.1$ kcal/mol. A similar approach has been used by others [44]. The coordination of zinc and calcium ions in the

pseudolysin structure was described by non-bonded energy terms in the calculations [44]. The MD simulations were performed with the AMBER 9.0 package [37] using the AMBER 2003 force field and a TIP3P water model. All molecular systems were solvated with a cubic box of water molecules and neutralized by counter ions. The Particle Mesh Ewald (PME) method was used for treatment of long range electrostatic interactions [46]. The non-bonded cut off radius was 10.0 Å, and the SHAKE option [47] was used to constrain bonds involving hydrogen atoms. The dielectric constant was 1, and all molecular systems were initially minimized by the conjugate gradient method and equilibrated for 200 ps of MD. During the equilibration, the temperature was gradually increased to 300 K and kept constant post equilibration. The MD simulations were run for a total of 24 ns. The time step during MD was 2 fs, and the non-bonded pair list was updated every 25 steps. Due to the +2 charge of the zinc ion and several surrounding anionic residues, the zinc atom and its ligated amino acids needed special treatment during MD in order to prevent distortion of the active site and the zinc coordination. Two histidines, a glutamic acid and a water molecule coordinate the zinc ion in the active site. Inhibitors usually replace this water molecule with a carboxylate, hydroxamate or phosphoramidate group as observed in the X-ray structure thermolysin-inhibitor complexes. Harmonic restraining force of 50 kcal/Å and distance restraints of 2.1 Å–2.5 Å was therefore used between the coordinating atoms of the hydroxamate and the zinc ion. Further, harmonic restraining force (50 kcal/Å) and a distance restraint (2.10 Å) were applied between zinc and its amino acid ligands: His 140 (atom NE2); His 144 (atom NE2) and Glu 164 (atom OE1). Similar approaches have also previously been used for calculations of zinc containing proteins [48,49]. The calculations were performed using a supercomputer with 1.3 GHz Itanium2 processors. Average pseudolysin-ligand complexes were calculated for the 400 ligand–pseudolysin coordinate sets obtained between 20 and 24 ns of MD using the ptraj package of the AMBER suite of programs.

Acknowledgement

We are grateful to Prof. Efrat Kessler, Tel Aviv University Sackler, Faculty of Medicine Goldschleger Eye Research Institute, Sheba Medical Center, Tel-Hashomer 52621, Israel for contributing with pseudolysin. The project was also supported by computer time from NOTUR – The Norwegian metacentre for computational science.

References

[1] N.D. Rawlings, A.J. Barrett, A. Bateman, MEROPS: the peptidase database, Nucleic Acids Res. 38 (Database issue) (2010) D227–D233.
[2] K. Inouye, N. Mazda, M. Kubo, Need for aromatic residue at position 115 for proteolytic activity found by site-directed mutagenesis of tryptophan 115 in thermolysin, Biosci. Biotechnol. Biochem. 62 (4) (1998) 798–800.
[3] M. Kusano, K. Yasukawa, K. Inouye, Insights into the catalytic roles of the polypeptide regions in the active site of thermolysin and generation of the thermolysin variants with high activity and stability, J. Biochem. 145 (1) (2009) 103–113.
[4] O.A. Adekoya, I. Sylte, The thermolysin family (M4) of enzymes: therapeutic and biotechnological potential, Chem. Biol. Drug Des. 73 (1) (2009) 7–16.
[5] L. Englert, A. Biela, M. Zayed, A. Heine, D. Hangauer, G. Klebe, Displacement of disordered water molecules from hydrophobic pocket creates enthalpic signature: binding of phosphonamidate to the S(1)'-pocket of thermolysin, Biochim. Biophys. Acta 1800 (11) (2010) 1192–1202.
[6] C.M. Salisbury, J.A. Ellman, Rapid identification of potent nonpeptidic serine protease inhibitors, Chembiochem: Eur. J. Chem. Biol. 7 (7) (2006) 1034–1037.
[7] F. Jin, O. Matsushita, S. Katayama, S. Jin, C. Matsushita, J. Minami, A. Okabe, Purification, characterization, and primary structure of Clostridium perfringens lambda-toxin, a thermolysin-like metalloprotease, Infect. Immun. 64 (1) (1996) 230–237.
[8] S. Miyoshi, S. Shinoda, Microbial metalloproteases and pathogenesis, Microbes Infect. 2 (1) (2000) 91–98.
[9] S. Miyoshi, Y. Sonoda, H. Wakiyama, M.M. Rahman, K. Tomochika, S. Shinoda, S. Yamamoto, K. Tobe, An exocellular thermolysin-like metalloprotease produced by Vibrio fluvialis: purification, characterization, and gene cloning, Microb. Pathog. 33 (3) (2002) 127–134.
[10] S. Miyoshi, H. Nakazawa, K. Kawata, K. Tomochika, K. Tobe, S. Shinoda, Characterization of the hemorrhagic reaction caused by Vibrio vulnificus metalloprotease, a member of the thermolysin family, Infect. Immun. 66 (10) (1998) 4851–4855.
[11] A. Vilcinskas, M. Wedde, Insect inhibitors of metalloproteinases, IUBMB life 54 (6) (2002) 339–343.
[12] C.Y. Hung, K.R. Seshan, J.J. Yu, R. Schaller, J. Xue, V. Basrur, M.J. Gardner, G.T. Cole, A metalloproteinase of Coccidioides posadasii contributes to evasion of host detection, Infect. Immun. 73 (10) (2005) 6689–6703.
[13] B. Altincicek, M. Linder, D. Linder, K.T. Preissner, A. Vilcinskas, Microbial metalloproteinases mediate sensing of invading pathogens and activate innate immune responses in the lepidopteran model host Galleria mellonella, Infect. Immun. 75 (1) (2007) 175–183.
[14] Z. Kuang, Y. Hao, B.E. Walling, J.L. Jeffries, D.E. Ohman, G.W. Lau, Pseudomonas aeruginosa elastase provides an escape from phagocytosis by degrading the pulmonary surfactant protein-A, PloS One 6 (11) (2011) e27091.
[15] C.A. Clark, L.K. Thomas, A.O. Azghani, Inhibition of protein kinase C attenuates Pseudomonas aeruginosa elastase-induced epithelial barrier disruption, Am. J. Respir. Cell. Mol. Biol. 45 (6) (2011) 1263–1271.
[16] A.W. Smith, B. Chahal, G.L. French, The human gastric pathogen Helicobacter pylori has a gene encoding an enzyme first classified as a mucinase in Vibrio cholerae, Mol. Microbiol. 13 (1) (1994) 153–160.
[17] K. Hiraga, S.S. Seeram, S. Tate, N. Tanaka, M. Kainosho, K. Oda, Mutational analysis of the reactive site loop of Streptomyces metalloproteinase inhibitor, SMPI, J. Biochem. 125 (1) (1999) 202–209.
[18] N.N. Sahney, J.T. Summersgill, J.A. Ramirez, R.D. Miller, Inhibition of oxidative burst and chemotaxis in human phagocytes by Legionella pneumophila zinc metalloprotease, J. Med. Microbiol. 50 (6) (2001) 517–525.
[19] Y. Komori, T. Nonogaki, T. Nikai, Hemorrhagic activity and muscle damaging effect of Pseudomonas aeruginosa metalloproteinase (elastase), Toxicon 39 (9) (2001) 1327–1332.
[20] A.O. Azghani, E.J. Miller, B.T. Peterson, Virulence factors from Pseudomonas aeruginosa increase lung epithelial permeability, Lung 178 (5) (2000) 261–269.
[21] R.W. Vandivier, V.A. Fadok, P.R. Hoffmann, D.L. Bratton, C. Penvari, K.K. Brown, J.D. Brain, F.J. Accurso, P.M. Henson, Elastase-mediated phosphatidylserine receptor cleavage impairs apoptotic cell clearance in cystic fibrosis and bronchiectasis, J. Clin. Investig. 109 (5) (2002) 661–670.
[22] K. Yanagihara, K. Tomono, Y. Kaneko, Y. Miyazaki, K. Tsukamoto, Y. Hirakata, H. Mukae, J. Kadota, I. Murata, S. Kohno, Role of elastase in a mouse model of chronic respiratory Pseudomonas aeruginosa infection that mimics diffuse panbronchiolitis, J. Med. Microbiol. 52 (Pt 6) (2003) 531–535.
[23] W.I. Mariencheck, J.F. Alcorn, S.M. Palmer, J.R. Wright, Pseudomonas aeruginosa elastase degrades surfactant proteins A and D, Am. J. Respir. Cell Mol. Biol. 28 (4) (2003) 528–537.
[24] A. Schmidtchen, E. Holst, H. Tapper, L. Bjorck, Elastase-producing Pseudomonas aeruginosa degrade plasma proteins and extracellular products of human skin and fibroblasts, and inhibit fibroblast growth, Microb. Pathog. 34 (1) (2003) 47–55.
[25] J.A. Hobden, Pseudomonas aeruginosa proteases and corneal virulence, DNA Cell Biol. 21 (5–6) (2002) 391–396.
[26] O.A. Adekoya, N.P. Willassen, I. Sylte, The protein-protein interactions between SMPI and thermolysin studied by molecular dynamics and MM/PBSA calculations, J. Biomol. Struct. Dyn. 22 (5) (2005) 521–531.
[27] O.A. Adekoya, N.P. Willassen, I. Sylte, Molecular insight into pseudolysin inhibition using the MM-PBSA and LIE methods, J. Struct. Biol. 153 (2) (2006) 129–144.
[28] M.T. Khan, R. Khan, Y. Wuxiuer, M. Arfan, M. Ahmed, I. Sylte, Identification of novel quinazolin-4(3H)-ones as inhibitors of thermolysin, the prototype of the M4 family of proteinases, Bioorg. Med. Chem. 18 (12) (2010) 4317–4327.
[29] M.T. Khan, O.M. Fuskevag, I. Sylte, Discovery of potent thermolysin inhibitors using structure based virtual screening and binding assays, J. Med. Chem. 52 (1) (2009) 48–61.
[30] S. Chaves, S. Marques, M.A. Santos, Iminodiacetyl-hydroxamate derivatives as metalloproteinase inhibitors: equilibrium complexation studies with Cu(II), Zn(II) and Ni(II), J. Inorg. Biochem. 97 (4) (2003) 345–353.
[31] S.M. Marques, E. Nuti, A. Rossello, C.T. Supuran, T. Tuccinardi, A. Martinelli, M.A. Santos, Dual inhibitors of matrix metalloproteinases and carbonic anhydrases: iminodiacetyl-based hydroxamate-benzenesulfonamide conjugates, J. Med. Chem. 51 (24) (2008) 7968–7979.
[32] M.A. Santos, S. Marques, D. Vullo, A. Innocenti, A. Scozzafava, C.T. Supuran, Carbonic anhydrase inhibitors: inhibition of cytosolic/tumor-associated isoforms I, II, and IX with iminodiacetic carboxylates/hydroxamates also incorporating benzenesulfonamide moieties, Bioorg. Med. Chem. Lett. 17 (6) (2007) 1538–1543.
[33] M.A. Santos, S.M. Marques, T. Tuccinardi, P. Carelli, L. Panelli, A. Rossello, Design, synthesis and molecular modeling study of iminodiacetyl monohydroxamic acid derivatives as MMP inhibitors, Bioorg. Med. Chem. 14 (22) (2006) 7539–7550.
[34] H.I. Park, S. Lee, A. Ullah, Q. Cao, Q.X. Sang, Effects of detergents on catalytic activity of human endometase/matrilysin 2, a putative cancer biomarker, Anal. Biochem. 396 (2) (2010) 262–268.

[35] R.A. Copeland, Enzymes: a Practical Introduction to Structure, Mechanisms and Data Analysis, second ed., John Wiley and Sons INC, 2000.
[36] R. Abagyan, T. Maxim, D. Kuznetsov, ICM-a new method for protein modelling and design: applications to docking and structure prediction from the distorted native conformation, J. Comp. Chem. 15 (5) (1994) 488–506.
[37] D.A. Case, T.E. Cheatham 3rd, T. Darden, H. Gohlke, R. Luo, K.M. Merz Jr., A. Onufriev, C. Simmerling, B. Wang, R.J. Woods, The Amber biomolecular simulation programs, J. Comput Chem. 26 (16) (2005) 1668–1688.
[38] A. Jakalian, B.L. Bush, D.B. Jack, C.I. Bayly, Fast, efficient generation of high-quality atomic charges. AM1-BCC model: I. Method, J. Comput Chem. 21 (2) (2000) 132–146.
[39] A. Jakalian, D.B. Jack, C.I. Bayly, Fast, efficient generation of high-quality atomic charges. AM1-BCC model: II. Parameterization and validation, J. Comput Chem. 23 (16) (2002) 1623–1641.
[40] C.I. Bayly, P. Cieplak, W.D. Cornell, P.A. Kollman, A well-behaved electrostatic potential based method using charge restraints for deriving atomic charges – the Resp model, J. Phys. Chem. 97 (40) (1993) 10269–10280.
[41] W.D. Cornell, P. Cieplak, C.I. Bayly, P.A. Kollman, Application of Resp charges to calculate conformational energies, hydrogen-bond energies, and free-energies of solvation, J. Am. Chem. Soc. 115 (21) (1993) 9620–9631.
[42] A. Vedani, YETI: an interactive molecular mechanics programme for small-molecules protein complexes, J. Comp. Chem. 9 (3) (1987) 269–280.
[43] A. Vedani, D.W. Huhta, A new force field for modeling metalloproteins, J. Am. Chem. Soc. 112 (12) (1990) 4759–4767.
[44] G.E. Terp, I.T. Christensen, F.S. Jorgensen, Structural differences of matrix metalloproteinases. Homology modeling and energy minimization of enzyme-substrate complexes, J. Biomol. Struct. Dyn. 17 (6) (2000) 933–946.
[45] R.H. Stote, M. Karplus, Zinc binding in proteins and solution: a simple but accurate nonbonded representation, Proteins 23 (1) (1995) 12–31.
[46] T. Darden, D. York, L. Pedersen, Particle mesh Ewald: an $N\cdot\log(N)$ method for Ewald sums in large systems, J. Chem. Phys. 98 (12) (1993) 10089–10092.
[47] W. F. v. Gunsteren, H.T.C. Berendsen, Algorithms for macromolecular dynamics and constraint dynamics, Mol. Phys. 34 (1977) 1311.
[48] S. Tate, A. Ohno, S.S. Seeram, K. Hiraga, K. Oda, M. Kainosho, Elucidation of the mode of interaction of thermolysin with a proteinaceous metalloproteinase inhibitor, SMPI, based on a model complex structure and a structural dynamics analysis, J. Mol. Biol. 282 (2) (1998) 435–446.
[49] Z.R. Wasserman, C.N. Hodge, Fitting an inhibitor into the active site of thermolysin: a molecular dynamics case study, Proteins 24 (2) (1996) 227–237.